

**Cosmological reionization after WMAP:
perspectives from PLANCK and future CMB missions**

C. Burigana¹, L.A. Popa^{1,2}, F. Finelli¹, R. Salvaterra³, G. De Zotti^{4,3}, and N. Mandolesi¹

¹INAF-CNR/IASF, Sezione di Bologna, via Gobetti 101, I-40129 Bologna (Italy)

²Institute for Space Sciences, Bucharest-Magurele R-76900 (Romania)

³SISSA, via Beirut 4, I-34014 Trieste (Italy)

⁴INAF - Osservatorio Astronomico di Padova, vicolo dell'Osservatorio 5, I-35122 Padova (Italy)

Abstract

The WMAP first year detection of a high redshift reionization through its imprints on CMB anisotropy T and TE mode angular power spectra calls for a better comprehension of the universe ionization and thermal history after the standard recombination. Different reionization mechanisms predict different signatures in the CMB, both in temperature and polarization anisotropies and in spectral distortions. The PLANCK capability to distinguish among different scenarios through its sensitivity to T, TE, and E mode angular power spectra is discussed. Perspectives open by future high sensitivity experiments on the CMB polarization anisotropy and spectrum are also presented.

1 Introduction

The accurate understanding of the ionization history of the universe plays a fundamental role in modern cosmology. The classical theory of hydrogen recombination for pure baryonic cosmolog-

ical models [1, 2], subsequently extended to non-baryonic dark matter models [3, 4, 5, 34] can be modified in various ways to take into account additional sources of photon and energy production able to significantly increase the ionization fraction, x_e , above the residual fraction ($\sim 10^{-3}$) after the standard recombination epoch at $z_{\text{rec}} \simeq 10^3$. These photon and energy production processes may leave imprints on the cosmic microwave background (CMB) providing a crucial “integrated” information on the so-called *dark* and *dawn ages*, i.e. the epochs before or at the beginning the formation of first stars and primeval galaxies, complementary to those obtained by the study of the diffuse backgrounds in other frequency bands and that are impossible or difficult to study with other direct astronomical observations.

Among the extraordinary results recently achieved by WMAP [7] the detection of a cosmological reionization at relevant redshifts [8] represents one of the new most remarkable discovery in the recent years. In spite of the uncertainty associated to the degeneracy [9] between the Thomson scattering optical depth, τ , and the spectral index of primordial perturbation, n_s , in CMB anisotropy data, a cosmological reionization at substantial redshifts is supported by the decrease of the temperature angular power spectrum at high multipoles and by an excess in the TE cross-power spectrum on large angular scale (multipoles $\ell \lesssim 7$) with respect to models with no-reionization or reionization with quite low (~ 0.05) values of τ . According to WMAP 1-yr data, the favourite values of τ are $\gtrsim 0.1$, with a current best fit of $\simeq 0.17$ based on the combination of WMAP with additional CMB anisotropy data at higher resolution and other kinds of astronomical observations (see, e.g., [10]). On the other hand, the details and the physical explanation of the cosmological reionization are still unclear.

Since the WMAP detection of the reionization at substantial redshifts, many models have been proposed and/or reconsidered to account for the measure of τ (see, e.g., [11]). Certainly, a significant contribution ($\simeq 0.05 - 0.07$) to the value of τ derives from the ionization, likely associated to photon production and hot gas ejection by primeval galaxies and quasars, at relatively low redshifts ($z \lesssim z_{\text{reion}}^{(2)} \simeq 5 - 7$) where direct observations of the Gunn-Peterson effect in quasars probe a high ionization level of the intergalactic medium. The remaining contribution ($\simeq 0.05 - 0.12$) to the observed value of τ should be provided by processes at higher redshifts. Although uncertain because of the possible non-uniformity of the ionization of the intergalactic medium, the indication of an increase of the Ly- α opacity for Gunn-Peterson tests toward some quasars at $z \sim 6$ [12, 13, 14] combined to the large WMAP value of τ suggests the possibility of a twice reionization, the first one at relevant redshifts, $z_{\text{reion}}^{(1)} \simeq 15$, possibly associated to Population III stars [15], or even at higher redshifts, $z_{\text{reion}} \gtrsim \text{some} \times 10$, in models involving a relevant photon production by particle decay, matter-antimatter annihilation, or black-hole evaporation and so on, followed by the subsequent reionization at $z \simeq z_{\text{reion}}^{(2)} \simeq 6$.

The reionization imprints on the CMB can be divided in three categories: *i*) decreasing of the power of CMB temperature anisotropy at large multipoles because of photon diffusion, *ii*) increasing of the power of CMB polarization and temperature-polarization cross correlation anisotropy at all multipoles with relevant features possibly more remarkable at low and middle multipoles according to the reionization epoch because of the delay of the effective last scattering surface, *iii*) generation of CMB Comptonization and free-free spectral distortions associated to the heating of the electron temperature of the intergalactic medium during the reionization

epoch. The imprints on CMB anisotropies are mainly dependent on the ionization history while CMB spectral distortions strongly depend also on the thermal history.

2 Observational perspectives from next and future experiments

The CMB anisotropy pattern is a single realization of a stochastic process and therefore it may be different from the average over the ensemble of all possible realizations of the given (true) cosmological model with given parameters. This translates into the fact that the $a_{\ell m}$ coefficients are random variables (possibly following a Gaussian distribution), at a given ℓ , and therefore their variance, C_ℓ , is χ^2 distributed with $2\ell + 1$ degrees of freedom. The relative variance δC_ℓ on C_ℓ is equal to $\sqrt{2/(2\ell + 1)}$ and is quite relevant at low ℓ s. This is the so-called “cosmic variance” which limits the accuracy of the comparison of observations with theoretical predictions. Another similar variance in CMB anisotropy experiments is related to the sky coverage since the detailed CMB anisotropy statistical properties may depend on the considered sky patch. This variance depends on the observed sky fraction, f_{sky} . At multipoles larger than $few \times 10^2$ the most relevant uncertainties are related to the experiment resolution and sensitivity. All these terms contribute to the final uncertainty on the C_ℓ according to [16]:

$$\frac{\delta C_\ell}{C_\ell} = \sqrt{\frac{2}{f_{\text{sky}}(2\ell + 1)}} \left[1 + \frac{A\sigma^2}{NC_\ell W_\ell} \right], \quad (1)$$

where A is the size of the surveyed area, σ is the rms noise per pixel, N is the total number of observed pixel, and W_ℓ is the beam window function. For a symmetric Gaussian beam $W_\ell = \exp(-\ell(\ell + 1)\sigma_B^2)$ where $\sigma_B = \text{FWHM}/\sqrt{8\ln 2}$ defines the beam resolution.

The two instruments at cryogenic temperatures on-board the ESA PLANCK satellite [17] (see also J. Tauber 2004, *this Meeting*), the Low Frequency Instrument (LFI; [18]; see also N. Mandolesi 2004, *this Meeting*) based on differential radiometers and the High Frequency Instrument (HFI; [19]) based on state-of-art bolometers at the focus of a 1.5 m aperture off-axis Gregorian telescope, will measure the CMB angular power spectrum with very high sensitivity up to multipoles $\ell \sim 1000 - 2000$ and an accurate control of the systematic effects. The two instruments will cover a frequency range from 30 to 857 GHz, necessary to accurately subtract the foreground contamination (see, e.g., G. De Zotti et al. 2004, *this Meeting*), with a (FWHM) resolution from $\sim 33'$ to $5'$ and a sensitivity from $\sim 15\mu\text{K}$ to the $\sim \mu\text{K}$ level in terms of antenna temperature on a square resolution element of with side of $\sim 10'$.

Fig. 1 compares PLANCK and WMAP final performances in terms of angular power spectrum recovery. Note that, at similar frequencies, the better sensitivity of PLANCK with respect to WMAP is mainly due to the lower level of the PLANCK instrumental noise achieved thanks to the better radiometer performance assured by the lower system temperature while at higher frequencies it derives from a combination of lower instrumental noise achieved thanks to high sensitivity bolometers and from the improving of resolution with the frequency for a given telescope size. The CMB angular power spectrum is reported without beam smoothing and by taking into account the beam window functions of several PLANCK frequency channels and of

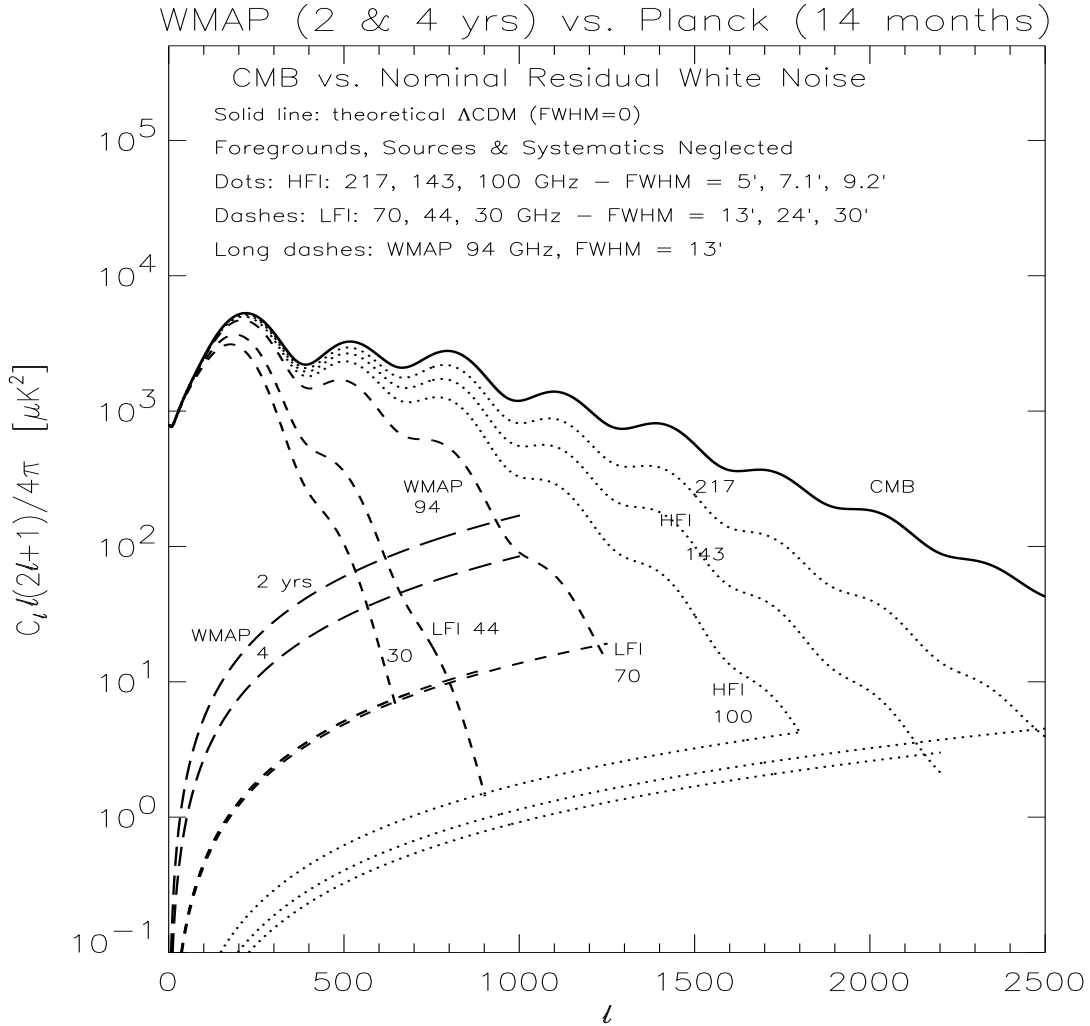


Figure 1: Comparison between PLANCK and WMAP resolution and sensitivity. For each considered frequency channel, the crossing between the CMB convolved angular power spectrum and the residual instrumental white noise angular power spectrum indicates the multipole value where the signal to noise ratio (ℓ by ℓ) is close to unity. Of course, binning the power spectrum on a suitable range of multipoles, as possible because of the smooth variation of C_ℓ with ℓ , will allow to recover the CMB power spectrum with a good accuracy also at multipoles comparable that those corresponding to the crossings between the noise and CMB power spectra reported in the figure (for example for the PLANCK channels at 70–100 GHz at $\ell \sim 1500$ a $\sim 3\%$ binning over ℓ allows to reduce the uncertainty on the C_ℓ recovery to $\sim 15\%$).

the highest WMAP frequency channel (which resolution is very close to that of the LFI 70 GHz channel). The corresponding angular power spectra of the residual nominal white noise (i.e. after the subtraction of the expectation value of the noise angular power spectrum) are also displayed. Similar considerations hold also for the measure of the polarization anisotropies (see, e.g., [20] for a summary of CMB polarization experiments). The sensitivity to the anisotropy measure of the Stokes parameters Q and U and of the polarization signal P ($P = \sqrt{Q^2 + U^2}$) is $\sim \sqrt{2} - 2$ times worse than that for the temperature anisotropy, the exact value depending on the detailed experimental strategy adopted to recover them from the combination of multi-beam data ¹. The low (of few–some %) polarization level predicted, and still only approximately measured [21], for the CMB anisotropy clearly calls for high sensitivity measurements which are less crucial for the temperature-polarization cross correlation (TE-mode) already measured by WMAP.

A quite accurate measure of the E-mode polarization is expected from the next WMAP data release, at least at degree scales, while the PLANCK instruments will have a good sensitivity to the polarization E-mode angular power spectrum also at scales of some arcminutes, the main limitation being represented by the foreground contamination, as shown in Fig. 2.

Thanks to the combination of temperature and polarization high quality data, PLANCK is expected to reduce the error bars in the recovery of the cosmological parameters at the level of *few %* or better and the final accuracy on a wide set of cosmological parameters will be largely independent [25] of the auxiliary information coming from other classes of astronomical observations which will be necessary to just remove some degeneracies intrinsic in the CMB information [9]. As an example, Fig. 3 compares the PLANCK sensitivity in constraining the Thomson optical depth and the density contrast with the sensitivity of WMAP, possibly combined with the Ly- α forest information (from [10]).

The PLANCK sensitivity and resolution will allow not only an extremely precise determination of the CMB angular power spectrum but also an accurate and multi-frequency imaging of the temperature anisotropy pattern on the whole sky and a quite accurate imaging of the polarization anisotropy pattern at least on some sky areas of particular sensitivity ² by combining the multi-frequency information. This is required for the study of the high order statistical properties of the CMB anisotropy at high resolution, crucial to test some cosmological scenarios predicting localized features (topological defects, some inflationary models, ...).

The detection of the polarization B-mode angular power spectrum is within the PLANCK capabilities at least over some suitable ranges of multipoles, but its accurate and exhaustive measure requires a new generation of dedicated experiments. As well known, the details of the reionization history strongly affect also the amplitude of the polarization B-mode angular power

¹For example, a ratio $\sqrt{2}$ can be easily obtained by taking into account that for differential radiometers the information from four receivers coupled to two feeds can be combined to derive a measure of a single temperature anisotropy data or of two (Q and U) polarization anisotropy data.

²Analogously to the WMAP survey, the scanning strategies foreseen for PLANCK will imply that the sky pixels on two areas (each of about 20–30 squared degrees) close to the ecliptic poles will be observed for a time significantly longer than the average resulting into a sensitivity significantly better (by about 5 times) than the average.

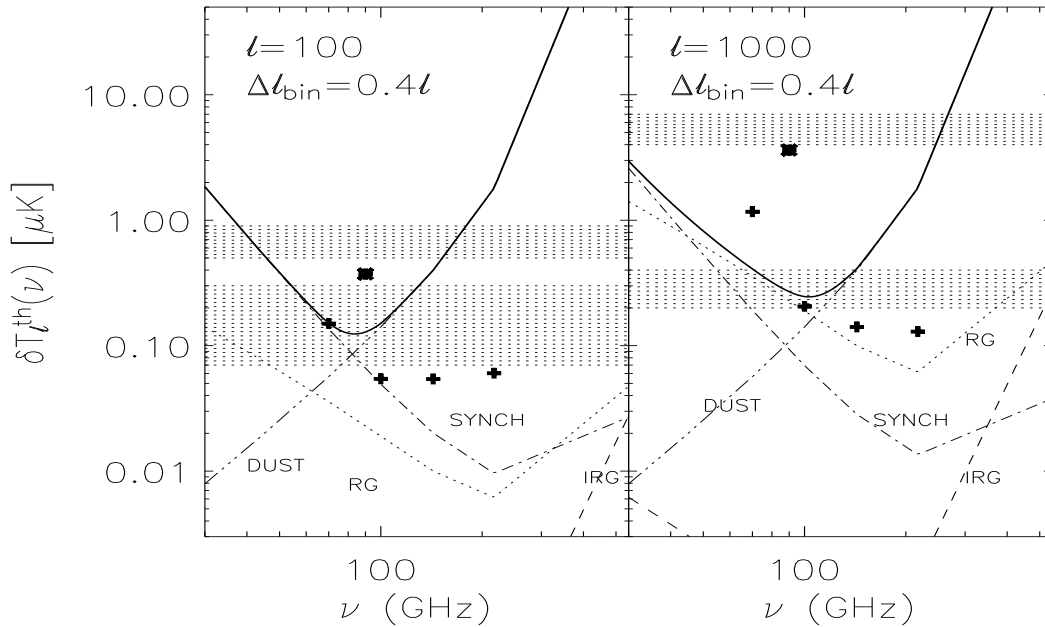


Figure 2: Typical predicted ranges for the CMB polarization angular power spectra (E-mode, upper dotted regions; B-mode, lower dotted regions) including the lensing [22] compared to the foreground contamination (radiogalaxies (dots) contribution (see [23] for a recent detailed study); the small contribution expected from infra-red galaxies (dashes); Galactic dust (three dots-dashes) and synchrotron (dot-dashes) emission [24, 20]) at two representative multipoles, as function of the frequency. We report the final sensitivity of WMAP at 94 GHz (asterisk) and of some PLANCK frequency channels (crosses) binned over a quite large range of multipoles.

spectrum, which depends on the amplitude of tensorial (gravitational waves) modes and, at small scales, on the lensing effect.

The cosmic variance uncertainty and the Galactic foreground contamination, quite relevant at low multipoles, decreases at middle and high multipoles. The atmospheric emission is expected to be less crucial for CMB polarization measurements than for anisotropy and spectrum ones. Therefore, ground-based observations ([26]; see, e.g., the VSA project ³) appear of particular interest for obtaining precise information at intermediate and high multipoles, thanks to the high sensitivity that could be reached with very long integration times and/or the use of a very large number of receivers. On the other hand, the space is the favourite site for the accurate measure of the CMB polarization at low and intermediate multipoles (see, e.g., the NASA Inflation Probe ⁴ of the Beyond Einstein program).

Fig. 4 reports the uncertainty (including cosmic variance and instrument sensitivity and resolution) in the recovery of the CMB polarization power spectra as achievable with a \sim yr full sky space mission discussed in the context of the call of mission themes of the ESA Cosmic Vision 2015-2025, by using the state of the art radiometers (right panel) and bolometers (left panel) at the focus of a set of four \sim 60 cm telescopes.

The comparison with Fig. 5 shows that, as long as foreground polarization anisotropies (and,

³<http://www.mrao.cam.ac.uk/telescopes/vsa/index.html>

⁴<http://universe.nasa.gov/program/inflation.html>

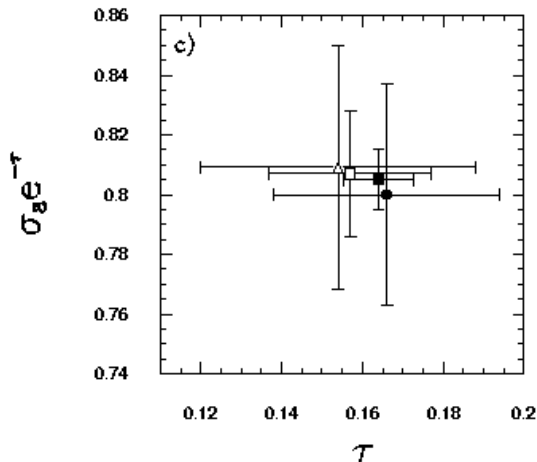


Figure 3: PLANCK sensitivity (filled square) in constraining the Thomson optical depth and the density contrast σ_8 compared with the sensitivity of WMAP 1-yr data (triangle), possibly combined with the Ly- α forest information (filled circle), and of WMAP 4-yr data (square). From [10].

in particular, the Galactic contamination) are accurately known and subtracted, the sensitivity levels presented above will allow to accurately measure also the B-mode or, depending on its intrinsic level, to set significant constraints on it.

The possibility to significantly improve our knowledge of the CMB spectrum with respect to the current observational status, in which the COBE/FIRAS data play the major role in constraining the CMB spectral distortions, has been recently addressed. In particular, two space mission proposals, the DIMES experiment [27], designed to reach an accuracy close to that of FIRAS but at centimeter wavelengths, and the FIRAS II experiment [28] which will allow a sensitivity improvement by a factor ~ 100 with respect to FIRAS, open the new perspective to detect CMB spectral distortion and not only to set constraints on them.

DIMES [27] is a space mission submitted to the NASA in 1995, designed to measure very accurately the CMB spectrum at wavelengths in the range $\simeq 0.33 - 15$ cm [27]. DIMES will compare the spectrum of each $\simeq 10$ degree pixel on the sky to a precisely known blackbody to precision of ~ 0.1 mK, close to that of FIRAS. The set of receivers is given from cryogenic radiometers with instrument emission cooled to 2.7 K operating at six frequency bands about 2, 4, 6, 10, 30 and 90 GHz using a single external blackbody calibration target common to all channels to minimize the calibration uncertainty. The DIMES design is driven by the need to reduce or eliminate systematic errors from instrumental artifacts. The DIMES sensitivity represents an improvement by a factor better than 300 with respect to previous measurements at centimeter wavelengths allowing a significant improvement of our knowledge on early dissipation processes and free-free distortions [29].

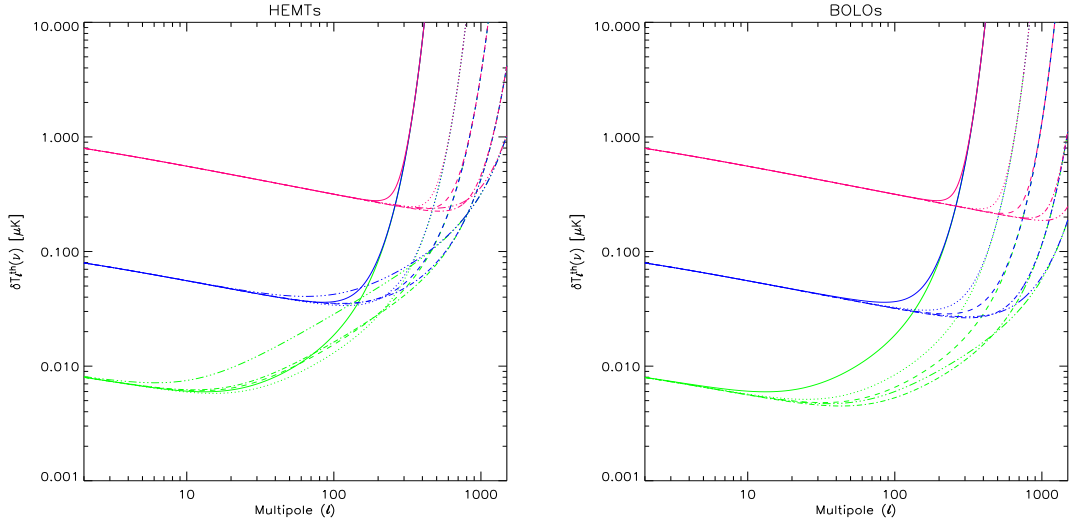


Figure 4: Residual uncertainty in the knowledge of the polarization angular power spectrum (in terms of $\delta T = (\ell(\ell+1)C_\ell/2\pi)^{0.5}$; thermodynamic temperatures are considered) including cosmic variance and detector sensitivity and resolution as in principle achievable by the next generation of CMB space missions. Right panel: the case of radiometer technology (typical sensitivity of $\simeq 0.1 - 0.25 \mu\text{K}$ on a pixel of $30'$ side). Left panel: the case of bolometer technology (typical sensitivity of $\simeq 0.04 - 0.12 \mu\text{K}$ on a pixel of $30'$ side). In each panel, the different lines refer to frequency channels at 32, 64, 94, 143, 217 GHz; at increasing frequency the error at high multipoles decreases because of the resolution increasing (from instance 1.09° to 0.16° (FWHM)) by using a given telescopes size. The cosmic variance has been computed by assuming, for simplicity, a constant polarization anisotropy level of 1, 0.1, and $0.01 \mu\text{K}$ in terms of δT (lines from the top to the bottom at low multipoles). Full sky coverage is assumed.

Fixsen and Mather [28] described the fundamental guidelines to significantly improve CMB spectrum measures at $\lambda \lesssim 1 \text{ cm}$. A great reduction of the residual noise of cosmic rays, dominating the noise of the FIRAS instrument, can be obtained by eliminating the data on-board co-add process or applying deglitching before co-adding, by reducing the size of the detectors and by using “spiderweb” bolometers or antenna-coupled micro-bolometers. They are expected to show a very low noise when cooled below 1 K while RuO sensors can reduce to 0.1 mK the read noise of thermometers. The Lagrangian point L2 of the Earth-Sun system is, of course, the favorite “site” for FIRAS II. Also, the calibration can be improved by order of magnitudes with respect to that of FIRAS by reducing the contribution to the calibrator reflectance of light from the diffraction at the junction between the calibrator and the horn. A complete symmetrical construction of the instrument is recommended. This allows the cross-check between calibrators and between calibrators and the sky and to realize “an end-to-end calibration and performance test before launch”. According to the authors, FIRAS II can be designed to have a frequency coverage from 60 to 3600 GHz (i.e. from 5 mm to $83 \mu\text{m}$) with a spectral resolution $\nu/\Delta\nu < 200$

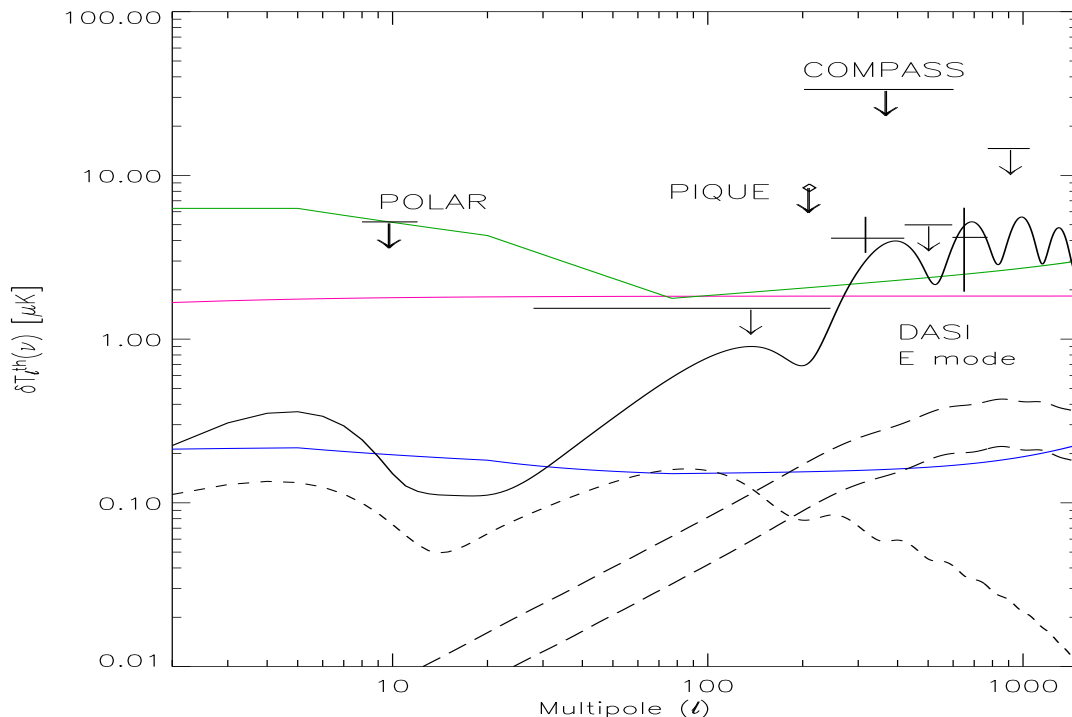


Figure 5: CMB polarization angular power spectra (E-mode: black solid line; B-mode: black dashes; B-mode from lensing: black long dashes) compared with reasonable predictions for the overall (Galactic plus extragalactic) foreground polarized angular power spectrum at 30 (green line), 100 (blue line) and 217 GHz (red line). The few recent upper limits and measures are reported for comparison [31, 32, 33, 21].

and sensitivity in each channel about 100 times better than that of FIRAS.

The combination of these two spectrum experiments open, at least in principle, the perspectives to detect and possibly measure spectral distortions imprinted by energy dissipations about 100 times smaller than those corresponding to the current upper limits set by FIRAS [30].

3 Reionization phenomenological models

The reionization process can be described phenomenologically in terms of injection of additional ionizing photons [34, 35, 36]. The ionization fraction of matter, $x_e = n_e/\bar{n}$, can be obtained from the balance between the processes of recombination and ionization:

$$\frac{dx_e}{dt} = -\alpha_{\text{rec}}(T)n_b x_e^2 + \varepsilon_i(z)(1 - x_e)H(z), \quad (2)$$

where $n_b(z)$ is and the mean baryonic density at the redshift z , T is the temperature of the plasma, $\alpha_{\text{rec}}(T) \simeq 4 \times 10^{-13} (T/10^4 K)^{-0.6} \text{ s}^{-1} \text{ cm}^{-3}$ is the recombination coefficient, and $\varepsilon_i(z)$ is the efficiency of the ionizing photon production giving the ionizing photon production rate

$dn_i/dt = \varepsilon_i(z)n_b(z)H(z)$; $H(z) = 1/t_{exp}$, where $t_{exp} = a/(da/dt)$ is the cosmic expansion time, a being here the cosmic scale factor.

The choice of the function $\varepsilon_i(z)$ allows to model the ionization history also in the presence of extra sources of ionizing photons (e.g. Ly- α and ionization photons from primavel stars, galaxies, and active galaxies, or from primordial black hole decays, electromagnetic cascades from particle release from topological defects or decay of super heavy dark matter, ...).

Assuming equilibrium between the recombination and the ionization process, for any given history of the plasma temperature the evolution of the ionization fraction is given by the solution of the simple second order equation obtained by the equality $dx_e/dt = 0$.

3.1 Late processes

For late processes, a simple expression describing a first reionization at relevant redshifts followed by a second reionization, possibly mimicking the model by Cen [15], has been proposed [37] in the form:

$$\varepsilon_i(z) = \varepsilon_0 \exp \left[-\frac{(z - z_{\text{reion}}^{(1)})^2}{(\Delta z_1)^2} \right] + \varepsilon_1 (1+z)^{-m} \Theta(z_{\text{reion}}^{(1)} - z); \quad (3)$$

here ε_0 , $z_{\text{reion}}^{(1)}$, and $\Delta z_1 \ll z_{\text{reion}}^{(1)}$ are free parameters describing the history of the first epoch of reionization which significantly decreases at $z > z_{\text{reion}}^{(1)}$; ε_1 , m , and (again) $z_{\text{reion}}^{(1)}$ are free parameters describing the history of the second epoch of reionization resulting into a increasing of $\varepsilon_i(z)$ with the time, being $\Theta(x)$ the step function.

Although quite weakly in this modelization, because of the dependence on the temperature as a power of $\simeq -0.6$ of the recombination coefficient, the thermal history influences the ionization fraction evolution. By using the matter temperature evolution $T(z) \simeq 270(1+z/100)^2$ K and modifying the ionization history in the CMBFAST code, the CMB angular power spectrum, in both temperature and polarization, has been computed [37] for some representative choices of the above free parameters. As shown by the authors for the case of the E-mode polarization power spectrum, the differences between different late reionization scenarios associated to very different parameters are of particular interest at relatively low multipoles. Provided that the contribution from the Galactic foregrounds, particularly relevant at these multipoles, could be accurately modeled, the difference between a scenario involving a single reionization at $z \simeq z_{\text{reion}}^{(2)}$ and scenarios involving a twice reionization could be detected by the PLANCK polarization accuracy.

The relevance of the detection of spectral distortions has been partially renewed [38] by the WMAP satellite discovery of a reionization phase at relevant redshifts.

The computation of the CMB spectral distortions associated to the reionization parametric model presented here is strictly related to the detailed description of the thermal history.

For these kinds of late processes, we assume here a matter thermal history similar to that reported by Cen [15]: a matter temperature T in approximate thermal equilibrium with the radiation field (i.e. equal to $T_0(1+z)$) at $z \gtrsim 27$; a linear dependence of $\log T$ on z at subsequent

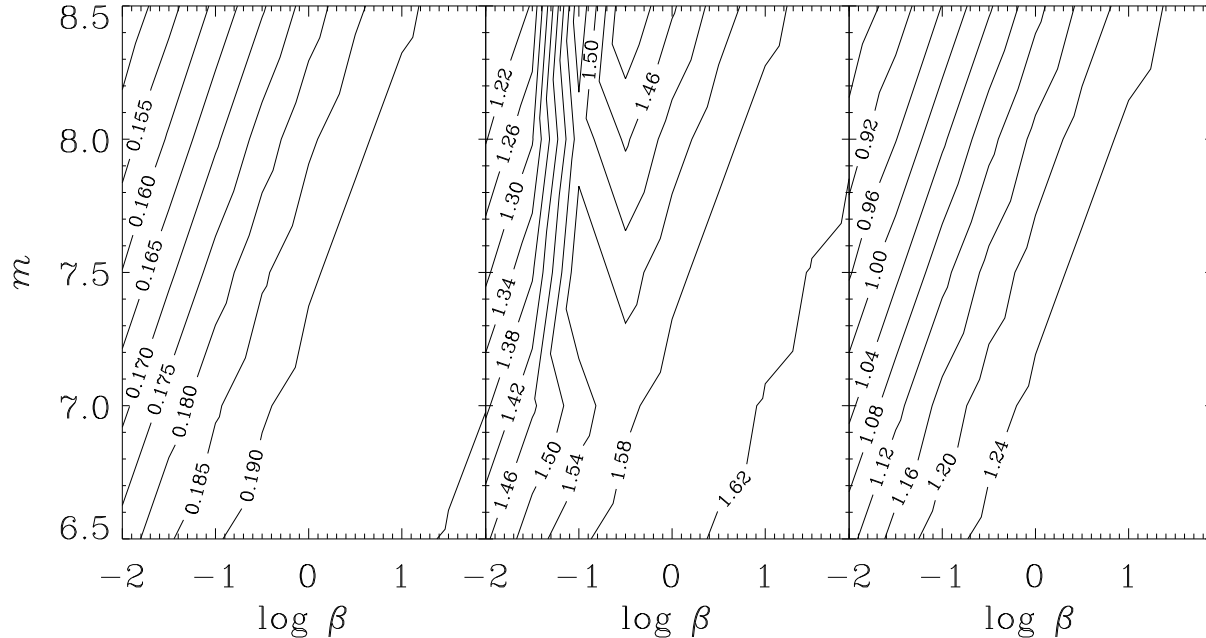


Figure 6: Contour plots of the optical depth and of the fractional injected energy associated to the Comptonization parameter as functions of β and m in the case of late reionization processes. Left panel: τ evaluated by integrating up to $z = 0$. Middle and right panels: $\Delta\epsilon/\epsilon_i \simeq 4u$ (in units of 10^{-6}) computed by integrating up to $z = 0$ and up to $z = 5$, respectively.

times to reach a temperature $T^{(1)}$ (assumed here 1.5×10^4 K for numerical estimates) at $z = z_{\text{reion}}^{(1)}$, kept then constant up to $z = z_{\text{reion}}^{(2)}$ when it rapidly increases up to a temperature $T^{(2)}$ (assumed here 2×10^4 K for numerical estimates) kept then constant up to low redshifts.

We have implemented this thermal history in the equilibrium evolution of the ionization fraction and then used these thermal and ionization histories to compute the Comptonization and free-free distortions as described in [39] by generalizing the code to include also the case of a Λ CDM model.

In Fig. 6 we report our contour plot results for the optical depth τ and the fractional energy injection associated to the Comptonization distortion as functions of the free parameters $\beta = \epsilon_1/10^9$ and m , by separately showing for $\Delta\epsilon/\epsilon_i$ the results of the integration up to $z = 0$ and up to $z = 5$ (of course, the difference between these results gives the fractional energy injected in the plasma at $z \leq 5$). For simplicity, we report here the results for an interval of β and m producing values of τ close to the current WMAP best fit [8]. Although a detailed computation requires to take into account the dependence of the ionization history on the matter temperature evolution, these results can be approximately rescaled to different values of $T^{(1)}$ and $T^{(2)}$ by considering the linear dependence of the Comptonization parameter on T . These predicted Comptonization distortions could be detected and possibly measured by an experiment with a sen-

sitivity like that of FIRAS II. Analogously to the case of the polarization anisotropy signatures, the difference between the Comptonization distortions by models involving a twice reionization (or a continuous reionization starting at $z \simeq z_{\text{reion}}^{(1)}$) and models with a single reionization at $z \simeq z_{\text{reion}}^{(2)}$ is comparable or above the FIRAS II sensitivity. The free-free distortion parameter y_B results to be too small, well below the DIMES sensitivity, and is not reported here ⁵.

3.2 High redshift processes

Models involving a substantial reionization at redshifts, $z \simeq z_{\text{reion}}$, much higher than $z_{\text{reion}}^{(1)} \sim 15$ can not be excluded by current data. A Gaussian parametric form

$$\varepsilon_i(z) = \xi \exp \left[-\frac{(z - z_{\text{reion}})^2}{(\Delta z)^2} \right], \quad (4)$$

quite similar to that assumed to describe the first reionization epoch for late processes, can be exploited in this context [37]; again ξ , z_{reion} , and Δz are free parameters describing the history of this high redshift reionization scenario. Assuming $\Delta z \ll z_{\text{reion}}$ implies the choice of a peak-like model. Again, it is necessary to add the evolution of the matter temperature which should peak at typical values of $T_p \approx (1 - 2) \times 10^4$ K. In [37] it is assumed an extremely short heating phase (δ -like) about z_{reion} . After the end of the heating phase the matter temperature is determined by the usual equation for the electron temperature evolution, dominated, at high redshifts, by the Compton cooling term. Therefore a set of two differential equations, one for the ionization fraction and the other for the matter temperature, describe the problem ⁶. This modified ionization history has been included in the CMBFAST code to compute the CMB angular power spectrum, in both temperature and polarization, for some representative choices of the above free parameters. As shown by the authors for the E-mode polarization angular power spectrum, the differences between different early reionization scenarios associated to different parameters and between them and a scenario involving a single late reionization at $z \simeq z_{\text{reion}}^{(2)}$ are relevant at low and also at middle multipoles, $\ell \sim \text{few} \times (10 - 100)$. This is of particular interest in the light of the PLANCK polarization accuracy in the multipole region of the CMB acoustic peaks where the contribution from the Galactic foregrounds is expected to significantly decrease with respect to the level it has at low multipoles.

For the study of the spectral distortions associated to early peak-like reionization processes, we have numerically integrated the differential equations for the ionization fraction and the matter temperature as described above. Differently from the δ -like assumption for the matter temperature during the heating phase about z_{reion} (that is not particularly critical for polariza-

⁵On the contrary, note that several specific physical models predict free-free distortion levels larger than those found in this simple modelization and clearly observable by a DIMES-like experiments (see, e.g., [30] and references therein).

⁶Simple approximate analytical solution can be used in the limit $\xi \ll 1$. We find also that the the system can be easily solved through a numerical integration. A simple backward differential scheme with a very small time step compared to the other relevant timescales does not introduce relevant errors in this context.

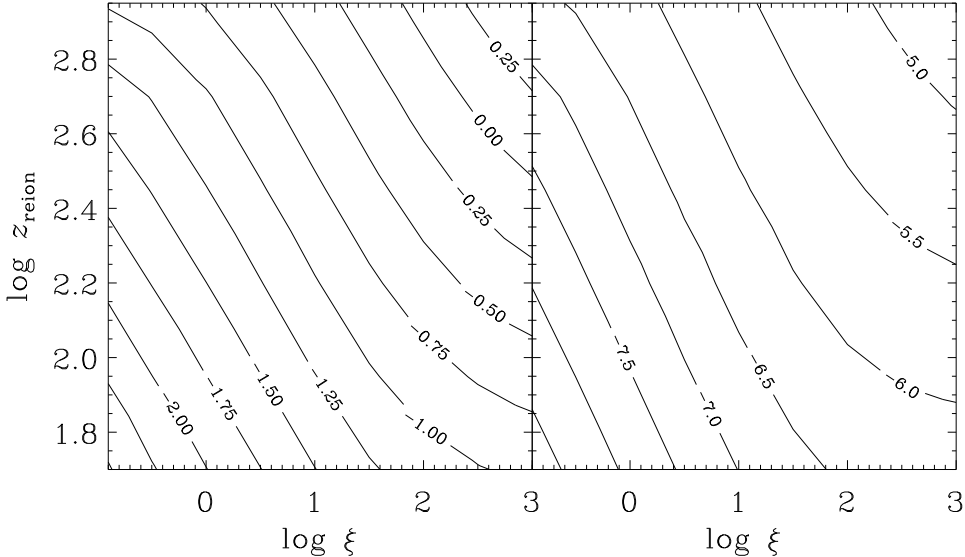


Figure 7: Contour plots of the optical depth, τ , (left panel) and of the fractional energy injection associated to the Comptonization parameter, $\Delta\epsilon/\epsilon_i \simeq 4u$, (right panel) as functions of ξ and z_{reion} in the case of early peak-like reionization processes (logarithmic scale).

tion anisotropy considerations) we adopt here a Gaussian parametric form

$$T(z) = T_p \exp \left[-\frac{(z - z_{\text{reion}})^2}{(\Delta z)^2} \right] \quad (5)$$

for the matter temperature during the heating phase (within a redshift interval $\simeq \pm 3\Delta z$ about z_{reion}) and then assume the usual temperature evolution equation, dominated by the Compton cooling term, at later epochs ($T_p = 1.5 \times 10^4$ K and $\Delta z = 0.025z_{\text{reion}}$ are adopted here for numerical estimates). It is in fact quite reasonable to assume a similar time dependence for both the efficiency of the ionizing photon production, $\epsilon_i(z)$, and the matter temperature during the active phase. We assume as initial conditions at the beginning of the heating/ionization phase the thermal equilibrium between matter and radiation and the residual ionization fraction obtained at the considered redshift from the standard recombination.

Finally, we have implemented the thermal and ionization history as described above in the code [39] for the computation of the Comptonization and free-free distortions.

In Fig. 7 we report our results in terms of contour plots for the optical depth τ and the fractional energy injection associated to the Comptonization distortion as functions of the free parameters ξ and z_{reion} . These results can be rescaled to different choices of T_p and Δz by using the approximate proportionality relations between τ and Δz and between u and $T_p\Delta z$ ⁷. Fig. 7 shows that a large region of the ξ and z_{reion} parameter space can be clearly ruled out

⁷In reality, for the lowest considered values of ξ ($\xi \approx 1$) we find an increasing of the Comptonization distortion with Δz larger by a factor $\approx 1.5 - 3$ than that suggested by the above proportionality and related to the different initial conditions (the process starts at earlier times) and to the different coupling between the ionization fraction and the matter temperature. We find that this holds also for the free-free distortion parameter y_B .

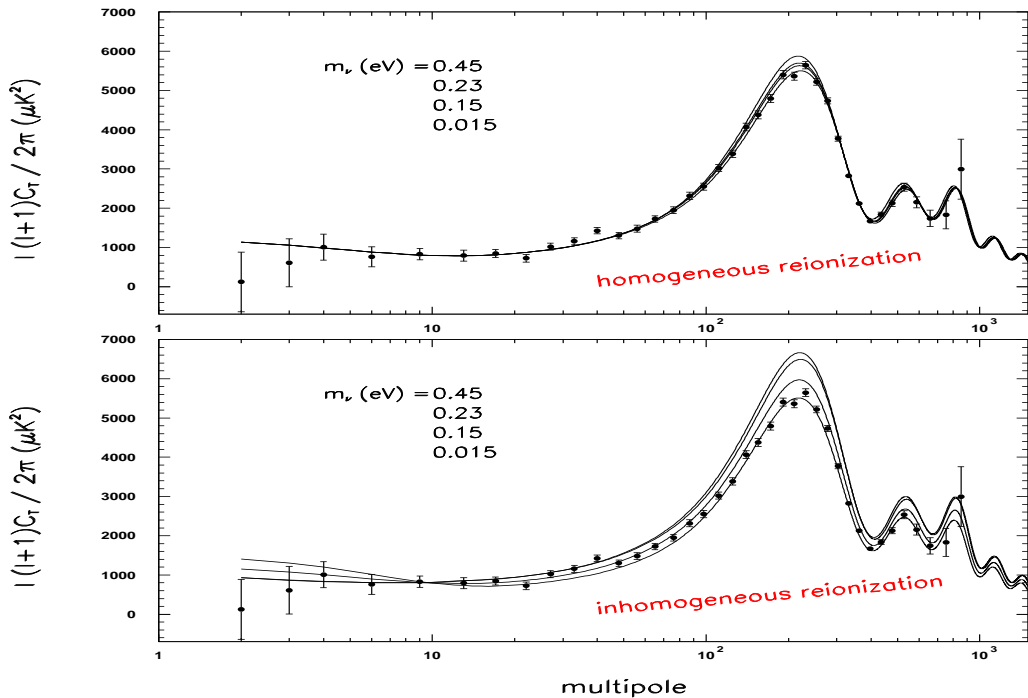


Figure 8: The CMB anisotropy power spectra for different neutrino masses considering (bottom panel) or not (top panel) the inhomogeneities of the reionization process.

by current WMAP data because of the violation of the limits on the optical depth. It is also remarkable that in the permitted region of ξ and z_{reion} (corresponding to $\tau \sim 0.1$) the model predicts values of fractional injected energy $\Delta\epsilon/\epsilon_i \simeq 4u \sim 10^{-6}$, again in principle measurable with the FIRAS II sensitivity. We find again values of free-free distortion parameter y_B too small with respect to the DIMES sensitivity ⁸.

To summarize, since it is plausible to assume peak matter temperatures $\gtrsim (1-2) \times 10^4$ K to have an efficient (late or early) reionization, values of $\Delta\epsilon/\epsilon_i \simeq 4u \sim (1-2) \times 10^{-6}$ should be considered as typical (lower limit) predictions for the Comptonization distortion associated to reionization scenarios compatible with the WMAP results [40].

4 Inhomogeneous reionization in the presence of massive neutrinos

As a specific example, we have investigated the role of a HDM component in the form of three massive neutrino flavors in the context of reionization scenarios. Assuming a flat background cosmology described by the best fit power law Λ CDM model with WMAP data ($\Omega_b h^2 = 0.024$,

⁸By considering higher matter temperature values (up to 6×10^4 K), we find only a weak dependence of y_B on T_p because the typical decreasing of y_B with T_p is approximately compensated by the increasing of the ionization fraction because of the decreasing of the recombination efficiency.

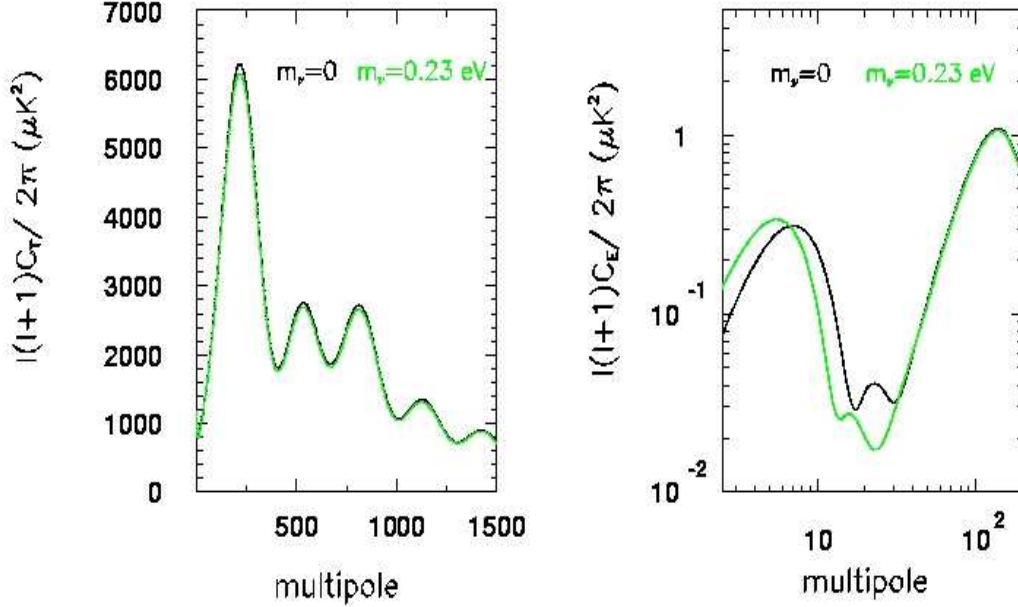


Figure 9: CMB temperature (left panel) and polarization (E-mode, right panel) anisotropy power spectra obtained for the above reionization model (including inhomogeneities) by considering or not the neutrino contribution for a specific value (25) of the reionization redshift. Note the sensitivity of polarization to the neutrino mass.

$\Omega_m h^2 = 0.14$, $h = 0.72$), we analyze the role of the neutrino mass for the properties of the gas in the intergalactic medium (IGM). We find that the temporal evolution of the hydrogen and helium ionization fractions is sensitive to the neutrino mass, with relevant implications for the CMB anisotropy and polarization angular power spectra.

The reionization is assumed to be caused by the ionizing photons produced in star-forming galaxies and quasars. This process depends on the evolution of the background density field that determines the formation rate of the bounded objects, the gas properties in the IGM and their feedback relation. At the redshift of collapse, the fraction of the mass of the gas in the virialized halos can be obtained if the probability distribution function of the gas overdensity is known. The temperature-density relation and the virial mass-temperature relation determines the connection between the gas density and the matter density at the corresponding scales [10]. During and after recombination, neutrinos with masses in eV range can have significant interactions with photons, baryons and cold dark matter particles via gravity only. The neutrino phase-space density is constrained by the Tremaine-Gunn criterion [41] that puts limits on the neutrino energy-density inside bounded objects. Neutrinos cannot cluster via gravitational instability on scales below

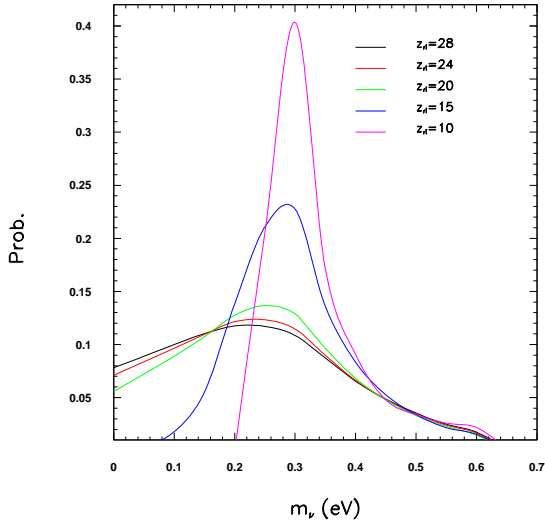


Figure 10: The probability density function of the neutrino masses (69% CL) as could be estimated by the PLANCK mission, using the CMB polarization measurements, for different reionization redshifts (fiducial model with $m_\nu = 0.23$ eV).

the free-streaming scale. The free-streaming distance determines the neutrino energy-density distribution inside the gravitationally collapsed objects [42], the temperature-density relation of the gas in the IGM and the hydrogen and helium ionization fractions.

In Fig. 8 we show the WMAP data compared with the CMB anisotropy power spectra obtained for different neutrino masses with (bottom) and without (top) considering the inhomogeneities of the reionization process. Fig. 9 compares the CMB temperature and polarization (E-mode) anisotropy power spectra obtained for the above reionization model (including inhomogeneities) by considering or not the neutrino contribution for a specific value of the reionization redshift. Clearly, polarization information greatly helps to distinguish between the two cases.

Finally, in Fig. 10 we show how in this specific reionization model the neutrino mass could in principle be constrained by PLANCK depending on the assumed reionization redshift. Note the improvement of the sensitivity to neutrino mass with the decreasing of the reionization redshift, as intuitive is because of the corresponding increase of the neutrino mass role.

5 Conclusion

The WMAP detection of a high redshift reionization calls for a better understanding of the physics of the reionization process. Different models predicts different imprints on the CMB in both temperature and polarization anisotropies while the presence of late spectral distortions (Comptonization like, with $\Delta\epsilon/\epsilon_i \sim \text{some} \times 10^{-6}$, and also free-free distortions with amplitudes

strongly dependent on the specific considered models) seems unavoidable for reasonable thermal histories in the context of reionization scenarios compatible with WMAP results.

Accurate measures of the CMB properties, such as those expected by the forthcoming PLANCK satellite and by future experiments will offer the opportunity to constrain the ionization and thermal history of the universe at moderate and high redshifts.

Acknowledgements

We thank L. Danese, L. La Porta, and L. Toffolatti for collaborations and discussions. We also thank L.-Y. Chiang, B. Ciardi, A. Ferrara, and P. Naselsky for useful conversations on the reionization history. The use of the CMBFAST code is acknowledged. Some of the results in this paper have been derived applying the HEALPix ⁹ (*Hierarchical Equal Area and IsoLatitude Pixelization of the Sphere*) by Górski et al. [43]) to the WMAP 1-yr data products. Some of the calculations presented here have been carried out on an alpha digital unix machine at the IFP/CNR in Milano by using some NAG integration codes. The staff of the LFI DPC in Trieste, where some simulations have been carried out, is acknowledged.

References

- [1] P.J.E. Peebles, 1968, ApJ, 153, 1.
- [2] Ya. B. Zel'dovich, V. Kurt, R.A. Sunyaev, 1968, Zh. Eksp. Theor. Phys., 55, 278.
- [3] N.A. Zabotin and P.D. Naselsky, 1982, Sov. Astron., 26, 272.
- [4] B.J.T. Jones and R. Wyse, 1985, A&A, 149, 144.
- [5] S. Seager, D.D. Sasselov, D. Scott, 2000, ApJS, 128, 407.
- [6] P.J.E. Peebles, S. Seager, W. Hu, 2000, ApJ, 539, L1.
- [7] C.L. Bennett et al., 2003, ApJS, 148, 1.
- [8] A. Kogut et al., 2003, ApJS, 148, 161.
- [9] J.R. Bond, R. Crittenden, R.L. Davis, G. Efstathiou, P.J. Steinhardt, 1994, PRL, 72, 13; J.R. Bond, R.L. Davis, P.J. Steinhardt, 1995, Astroph. Lett. and Comm., 32, 53; G. Efstathiou and J.R. Bond, 1999, MNRAS, 304, 75.
- [10] L.A. Popa, C. Burigana, N. Mandolesi, 2004, NA, 9, 189.
- [11] R. Bean, A. Melchiorri, J. Silk, 2003, Phys. Rev. D 68, 083501.
- [12] R.H. Becker et al., 2001, AJ, 122, 2850.

⁹<http://www.eso.org/science/healpix/>

- [13] X. Fan et al., 2002, AJ, 123, 1247.
- [14] X. Fan et al., 2004, AJ, in press, astro-ph/0405138.
- [15] R. Cen, 2003, ApJ, 591, 12.
- [16] L. Knox, 1995, Phys. Rev. D 48, 3502.
- [17] J.A. Tauber, 2000, in *The Extragalactic Infrared Background and its Cosmological Implications*, Proc. of the IAU Symposium, Vol. 204, eds. M. Harwit and M. Hauser.
- [18] N. Mandolesi et al., 1998, PLANCK LFI, A Proposal Submitted to the ESA.
- [19] J.L. Puget et al., 1998, HFI for the PLANCK Mission, A Proposal Submitted to the ESA.
- [20] G. De Zotti, 2002, in *Astrophysical Polarized Background*, eds. S. Cecchini et al., AIP Conf. Proc. 609, pg. 295.
- [21] J. Kovac et al., 2002, Nature, 420, 772.
- [22] M. Zaldarriaga and U. Seljak, 1998, Phys. Rev. D 58, 023003.
- [23] M. Tucci, E. Martinez-Gonzalez, L. Toffolatti, J. Gonzalez-Nuevo, G. De Zotti, 2004, MNRAS, 349, 1267.
- [24] C. Burigana and L. La Porta, 2002, in *Astrophysical Polarized Background*, eds. S. Cecchini et al., AIP Conf. Proc. 609, pg. 54.
- [25] L.A. Popa, C. Burigana, N. Mandolesi, 2001, ApJ, 558, 10.
- [26] M. Hobson, *High-resolution CMB interferometry*, Talk at *The Future of CMB*, Meeting at TAC, Copenhagen (NL), November 2003.
- [27] A. Kogut, 1996, *Diffuse Microwave Emission Survey*, in XVI Moriond Astrophysics meeting *Microwave Background Anisotropies*, March 16-23, Les Arcs, France, astro-ph/9607100.
- [28] D.J. Fixsen and J.C. Mather, 2002, ApJ, 581, 817.
- [29] C. Burigana and R. Salvaterra, 2003, MNRAS, 342, 543.
- [30] C. Burigana and R. Salvaterra, 2003, astro-ph/0309509.
- [31] C.W. O'Dell, B.G. Keating, A. de Oliveira-Costa, M. Tegmark, P.T. Timbie, 2003, Phys. Rev. D. 68, 42002.
- [32] M.M. Hedman et al., 2002, ApJ, 573, L73.
- [33] P.C. Farese et al., 2004, ApJ, 610, 625.
- [34] P.J.E. Peebles, S. Seager, W. Hu, 2000, ApJ, 539, L1.

- [35] A.G. Doroshkevich, P.D. Naselsky, 2002, *Phys. Rev. D* 65, 13517.
- [36] A.G. Doroshkevich, I.P. Naselsky, P.D. Naselsky, I.D. Novikov, 2003, *ApJ*, 586, 709.
- [37] P. Naselsky and L.-Y. Chiang, 2004, *MNRAS*, 347, 795.
- [38] A. Kogut, 2003, in the Proc. of *The Cosmic Microwave Background and its Polarization*, New Astronomy Reviews, eds. S. Hanany and K.A. Olive, Volume 47, Issues 11-12, pg. 945.
- [39] C. Burigana, G. De Zotti, L. Danese, 1995, *A&A*, 303, 323.
- [40] C. Burigana, F. Finelli, R. Salvaterra, L.A. Popa, N. Mandolesi, 2004, in *Research Signpost, Recent. Res. Devel. Astronomy & Astrophys.*, Vol. 2, 59.
- [41] S. Tremaine and J.E. Gunn, 1979, *PRL*, 42, 407.
- [42] L.A. Popa, C. Burigana, N. Mandolesi, 2002, *ApJ*, 580, 16.
- [43] K.M. Górski, E. Hivon, B.D. Wandelt, 1999, in Proc. of the *MPA/ESO Conference on Evolution of Large-Scale Structure: from Recombination to Garching*, eds. A.J. Banday, R.K. Sheth, L. Da Costa, pg. 37, astro-ph/9812350.